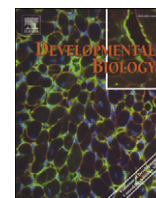


Contents lists available at [ScienceDirect](http://www.sciencedirect.com)

## Developmental Biology

journal homepage: [www.elsevier.com/developmentalbiology](http://www.elsevier.com/developmentalbiology)

## Germ-line mitochondria exhibit suppressed respiratory activity to support their accurate transmission to the next generation

Naomi Kogo, Akira Tazaki<sup>1</sup>, Yasuhiro Kashino, Keisuke Morichika<sup>2</sup>, Hidefumi Oori,  
Makoto Mochii, Kenji Watanabe<sup>\*</sup>

Graduate School of Life Science, University of Hyogo, 3-2-1 Koto, Kamigori, Akou-gun, Hyogo 678-1297, Japan

## ARTICLE INFO

## Article history:

Received for publication 3 September 2010

Revised 21 October 2010

Accepted 10 November 2010

Available online 26 November 2010

## Keywords:

Mitochondria

Germ plasm

Oocyte

ATP synthase

Respiration

## ABSTRACT

Mitochondria are accurately transmitted to the next generation through a female germ cell in most animals. Mitochondria produce most ATP, accompanied by the generation of reactive oxygen species (ROS). A specialized mechanism should be necessary for inherited mitochondria to escape from impairments of mtDNA by ROS. Inherited mitochondria are named germ-line mitochondria, in contrast with somatic ones. We hypothesized that germ-line mitochondria are distinct from somatic ones. The protein profiles of germ-line and somatic mitochondria were compared, using oocytes at two different stages in *Xenopus laevis*. Some subunits of ATP synthase were at a low level in germ-line mitochondria, which was confirmed immunologically. Ultrastructural histochemistry using 3,3'-diaminobenzidine (DAB) showed that cytochrome c oxidase (COX) activity of germ-line mitochondria was also at a low level. Mitochondria in one oocyte were segregated into germ-line mitochondria and somatic mitochondria, during growth from stage I to VI oocytes. Respiratory activity represented by ATP synthase expression and COX activity was shown to be low during most of the long gametogenetic period. We propose that germ-line mitochondria that exhibit suppressed respiration alleviate production of ROS and enable transmission of accurate mtDNA from generation to generation.

© 2010 Elsevier Inc. All rights reserved.

## Introduction

The mitochondrial genome in animal cells has been conserved throughout evolution for more than 800 million years; all mtDNAs in metazoic cells have a similar length, from 13 to 19 kbp, containing 37 genes (Saccone et al., 2002). Mitochondria are accurately transmitted to the next generation. However, mitochondria are organelles responsible for most ATP production. They are best known for housing the oxidative phosphorylation (OXPHOS) machinery. Mitochondria generate the majority of cellular ROS, which may impair mtDNA. In somatic cells, the mitochondrial genome is vulnerable to rapid accumulation of deleterious mutations during an individual animal's lifetime (Wallace et al., 1995).

Several investigators proposed a bottleneck hypothesis to explain the strict limitation of deleterious mutations in the mitochondrial genome through generations (Bergstrom and Pritchard, 1998; Hauswirth and Laipis, 1982). However, the mechanism remains

contentious. It is thought that the bottleneck occurs during embryonic development, as a result of a marked reduction in germ-line mtDNA copy number (Cree et al., 2008). Otherwise, it occurs without a reduction in germ-line mtDNA content (Cao et al., 2007; Wai et al., 2008), and the mtDNA genetic bottleneck results from replication of a subpopulation of mtDNA (Wai et al., 2008). The selection of mitochondria may be necessary for the transmission of intact mitochondria to the next generation. We have hypothesized that inherited mitochondria (germ-line mitochondria) are distinct from those of non-inherited ones (somatic mitochondria). This is the first report to compare directly germ-line mitochondria with somatic ones.

Germ plasm is the cytoplasm found in germ-line cells of some animals, including *Xenopus laevis*. Germ plasm contains the molecules and organelles that probably function in the differentiation and maintenance of germ-line cells (Kloc et al., 2001). A remarkably large number of mitochondria are found in germ plasm. They are parceled out to a small number of cells together with other components during development and are finally transmitted to the next generation.

The process of oocyte growth in *Xenopus* is divided in 6 stages (Dumont, 1972). In stage I oocytes, germ plasm is called mitochondrial cloud or Balbiani body, which contains a large number of mitochondria (Heasman et al., 1984). The space between mitochondria is filled with mitochondrial cement, which is probably precursor of germinal granules. That is, most mitochondria in mitochondrial cloud are germ-line. In stage VI oocytes, small patches of germ plasm

<sup>\*</sup> Corresponding author. Fax: +81 791 58 0187.E-mail addresses: [tazaki@mpi-cbg.de](mailto:tazaki@mpi-cbg.de) (A. Tazaki), [keisuke\\_morichika@rikkyo.ac.jp](mailto:keisuke_morichika@rikkyo.ac.jp) (K. Morichika), [kirowato@sci.u-hyogo.ac.jp](mailto:kirowato@sci.u-hyogo.ac.jp) (K. Watanabe).<sup>1</sup> Present address: Center for Regenerative Therapies Dresden, University of Technology Dresden, Tatzberg 47/49, 01307 Dresden, Germany.<sup>2</sup> Present address: Graduate School of Life Science, Faculty of Science, Rikkyo University, 3-34-1 Nishi-Ikebukuro, Toshima-ku, Tokyo 171-8501, Japan.

with mitochondria are localized at the cortex of the vegetal hemisphere. In the animal hemisphere, there are a large number of mitochondria, which are somatic mitochondria distributed to somatic cells (Tourte et al., 1984). That is, most mitochondria in stage VI are somatic.

We compared the protein profiles of the mitochondrial cloud fraction from stage I oocytes and mitochondria fraction from stage VI oocytes. We found that ATP synthase was at a lower level in germ-line mitochondrial than somatic ones. In the most of oogenesis, the expression of ATP synthase in germ-line mitochondria was at a low level. COX as well as ATP synthase is one of major components of the respiratory chain. The COX activity was also suppressed in most of oogenetic period. It is important for animals to suppress respiratory activity of germ-line mitochondria during the long oogenetic period. We propose that suppressed respiration of germ-line mitochondria avoids producing ROS and enables the accurate transmission of mtDNA from generation to generation.

## Materials and methods

### Oocytes

Ovary was surgically obtained from a mature female, and stage VI oocytes were defolliculated by 0.2% collagenase (Wako) treatment (Cohen and Pante, 2005), with modifications. Stage I oocytes were isolated from froglets (body length 4–6 cm) as for stage VI oocytes.

### Purification of stage VI oocyte mitochondria

We modified the protocol of (Bogenhagen et al., 2003; Wu and Dawid, 1972). All steps in the purification of mitochondria were conducted at 0–5 °C. The following buffers were used: TE (10 mM Tris–HCl, pH7.5, 1 mM EDTA); 0.25 M TES, 1 M TES, and 1.5 M TES were TE with 0.25 M, 1 M, and 1.5 M sucrose, respectively; and KMTD (0.125 M KCl, 7 mM MgCl<sub>2</sub>, 30 mM Tris–HCl, pH 8.0, 0.03 mM dithiothreitol). Oocytes were homogenized in 0.25 M TES. The homogenate was filtered through cheesecloth to remove most of stage I–III oocytes. Mitochondria fraction was prepared by some rounds of centrifugation and resuspended in 1 ml of KMTD. The resuspended mitochondria were layered over two preformed sucrose step gradients containing 1.2 ml of 1 M TES over 1.2 ml of 1.5 M TES in Ultracentrifuge tubes. Gradients were spun at 92,600×g (BECKMAN TL-100 Ultracentrifuge, rotor TLA 100.3) for 30 min to sediment mitochondria to the 1 M/1.5 M TES interface. The mitochondrial layer was gently removed, leaving the 1.5 M TES layer behind. Mitochondria were diluted with 0.25 M TS (0.25 M TES without EDTA) buffer and repelleted and resuspended in 0.25 M TS.

### Differential absorption spectrum (reduced - oxidized)

Differential absorption spectrum of air-oxidized and sodium dithionite (final concentration, 10 mM) reduced mitochondria of stage VI oocytes (25 mg/ml) was obtained using a homemade spectrophotometer, which was used for mammalian mitochondria (Takahashi et al., 2005).

### Purification of mitochondrial cloud of stage I oocytes

We modified the protocol of Chan et al. (1999). 0.1 ml of stage I oocytes isolated by collagenase treatment was transferred to an 1.5 ml microtube and was homogenized on ice with plastic bar. The homogenate was diluted with 0.25 M TES up to 0.8 ml, and it was placed on top of centrifuge tube containing a step gradient of 1 ml of 1.5 M TES, 0.6 ml of 0.4 M TES, and 0.6 ml of 0.25 M TES. Centrifugation was carried out for 45 min at 110,000×g. After fractionation, a layer of grayish “fluffy” material obtained near the middle layer was

collected as mitochondrial cloud fraction. The mitochondrial cloud fraction was diluted with 0.25 M TS and pelleted and resuspended in 0.25 M TS buffer.

### Protein analysis

Protein separation was carried out by using a 18–24% gradient acrylamide gel containing 6 M urea (Kashino et al., 2001). Mitochondria of stage VI oocytes (20 µg of protein) or mitochondrial cloud of stage I oocytes (40 µg of protein) were mixed with an equal amount of denaturing solution and subjected to electrophoresis without further boiling (Kashino, 2003). For the N-terminal sequencing, proteins were blotted onto the PVDF membrane (Amersham Pharmacia Biotech) after electrophoresis. The proteins on the membrane were stained by 0.1% Amido Black-10B (Nacalai Tesque, Kyoto, Japan) in a solution containing 10% methanol and 2% acetic acid and were then treated overnight with 0.6 N HCl at room temperature for the deblockage of the formylated N-terminus (Ikeuchi et al., 1989). The amino acid sequences of proteins were determined by a polypeptide sequencer (Shimadzu PSQ-1 protein sequencer; Simazu, Kyoto, Japan). Determined amino acid sequences were identified by BLAST search (Altschul et al., 1997).

### Production of antibodies

Overall procedures followed (Orie et al., 2002). F<sub>0</sub>-b (xL058e21), F<sub>1</sub>-β (xL043e02), GOT (xL026b18), and MDH (xL091c04) cDNAs were characterized using the NIBB/NIG/NBRP *X. laevis* EST database (XDB3; <http://xenopus.nibb.ac.jp/>). Almost full length of each protein was used as antigen. For F<sub>0</sub>-b, the cDNA corresponding to the sequence 50–250 a.a. was amplified by polymerase chain reaction (PCR) using forward primer 5'-atagcatgcgtccgttttggttgatccct-3', containing a SphI site and reverse primer 5'-cgcgctgacttaactctgtgtgcagt-3' containing a SalI site. The PCR product was cloned into the pQE30 vector (Qiagen) using these sites. The construct was introduced into *Escherichia coli* strain XL1Blue (Stratagene). This region of F<sub>0</sub>-b was expressed as a fusion protein with dihydrofolate reductase and histidine tag, and purified using a Ni-NTA resin column according to the manufacturer's protocol (Qiagen). The protein was dialyzed against water, lyophilized, and dissolved in phosphate-buffered saline (PBS). An appropriate volume of this solution was emulsified with Freund's adjuvant complete or incomplete (Sigma) and injected into Balb/c mice or Japanese white rabbits at intervals of 1 month. For F<sub>1</sub>-β, GOT, MDH, the cDNA corresponding to the sequence 9–525 a.a., 28–427 a.a., 1–338 a.a. was amplified by PCR using forward primer 5'-atagcatgctctgctgggctctgcgggct-3', 5-atagagctctctggtgtctcatgttgag-3', 5'-atagatgcctggttctctgcgcagcaga-3', and reverse primer 5'-gcgaagcttatgagtctctctgcgagtt-3', 5'-cgcaagcttcttgggtcacttggtgaat-3', 5'-cgcaagcttcacttcggctcttgatgaat-3', respectively. All other procedures for preparation of the antisera against these proteins were same as those for F<sub>0</sub>-b.

### Western blotting

Mitochondria of stage VI oocytes (1 µg of protein) or mitochondrial cloud of stage I oocytes (2 µg of protein) were mixed with an equal amount of denaturing solution. Proteins were separated by Laemmli's SDS-PAGE and blotted onto PVDF membrane after electrophoresis. The membrane was probed with primary antisera (anti F<sub>0</sub>-b 1:1500, F<sub>1</sub>-β 1:3000, GOT 1:6000, MDH 1:1000). After washing, peroxidase-conjugated goat anti-mouse IgG (Bio-Rad) was used as secondary antibody, and detection was enhanced by super-signal CL-HRP substrate (PIERCE). For stripping primary and secondary antibodies from blots, the membrane was incubated in stripping buffer (62.5 mM Tris–HCl, pH 6.7, 2% SDS, 0.1 M 2-mercaptoethanol)

at 60 °C for 20 min and washed extensively with TPBS (PBS containing 0.1% Triton X-100) before reblocking and reprobing.

### Immunostaining

For sections, ovary dissected from mature female was fixed in Bouin's fluid for overnight at room temperature. Immunostaining of paraffin-embedded section was performed as described previously (Ito et al., 2001). Mouse antiserum against F<sub>0</sub>-b and rabbit antiserum against GOT as the primary antibodies were used at 500- and 1500-fold dilution, respectively. Sections were washed in TPBS and reacted with Alexa-488 conjugated anti-mouse IgG and Cy3-conjugated anti-rabbit IgG (Molecular Probes). After washing in TPBS, they were mounted in 50% glycerol and observed under a fluorescent microscope BX60 (Olympus).

### Preparation for electron microscopy

Small pieces of ovary containing stage I–II oocytes were dissected from froglets. They were fixed in 2% glutaraldehyde and 2% paraformaldehyde in 0.1 M phosphate buffer (pH 7.4) including 25 mM sucrose (sPB). After fixation, they were washed for 1 h at RT in sPB and postfixed in 2% OsO<sub>4</sub> in 0.1 M cacodylate buffer and dehydrated in a graded series of alcohols, passed to propylene oxide and embedded in Spurr resin (Polysciences). Ultrathin sections (80 nm) were stained with 2% uranyl acetate and Reynald's lead citrate for 5 min and observed under electron microscope (JEM-1200 EX 11, JEOL).

### Assay of COX activity

We modified the protocol of Seligman et al. (1968). Small pieces of ovary of froglets and the defolliculated stage III–VI oocytes were fixed in 1% paraformaldehyde in sPB for 90 min at 4 °C. After fixation, they were washed for 1 h at 4 °C in sPB, then they were incubated in 2 mg/ml DAB/sPB for 60 min at 22 °C. The reaction was stopped in chilled sPB for 60 min at 4 °C. Controls were prepared by preincubating the samples in sPB containing 1 μM KCN for 10 min at 22 °C, and then incubating in 2 mg/ml DAB sPB with 1 μM KCN 1 h at 22 °C. After DAB reaction, specimens were refixed in 2% glutaraldehyde and 2% paraformaldehyde in sPB and postfixed in 2% OsO<sub>4</sub> in 0.1 M cacodylate buffer and dehydrated and embedded as mentioned above. Ultrathin sections (80 nm) were stained with Reynald's lead citrate for 5 min and observed under electron microscope.

## Results

### Subunits of ATP synthase are low at the protein level in mitochondria of stage I oocytes

In order to compare the protein profiles between germ-line and somatic mitochondria, we chose oocytes at two different stages as sources for mitochondria. For somatic mitochondria, we used stage VI oocytes, since the majority of the mitochondria at this stage are distributed to somatic cells (Tourte et al., 1984). Differential absorption spectrum (reduced-oxidized) of the purified mitochondria from this stage gave peaks at 552, 563, and 604 nm, which are ascribed to cytochromes *c* (*c*<sub>1</sub>), *b*, and *a*, respectively (Fig. 1A). The spectral characteristics of the purified mitochondria indicated that preparation of mitochondria was not significantly contaminated by any other organelle. For germ-line mitochondria, we collected the mitochondrial cloud: the germ plasm of stage I oocytes. The mitochondria from mitochondrial cloud preparation could not be purified further. Mitochondrial cloud was contaminated by other organelles (Fig. 1B).

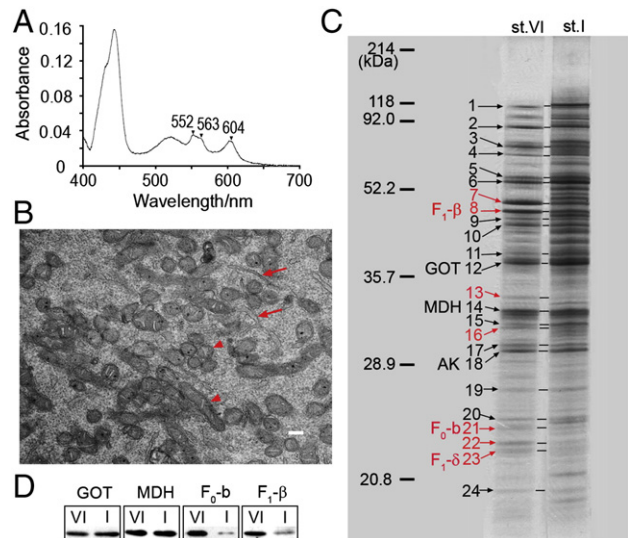


**Fig. 1.** Comparison between mitochondria of stage VI oocytes and mitochondrial cloud of stage I oocytes. (A, B) Purity of stage VI and I samples. High purity of stage VI oocyte mitochondria was shown by differential absorption spectrum giving peaks at 552, 563, and 604 nm ascribed to cytochromes *c* (*c*<sub>1</sub>), *b*, and *a*, respectively (A). Routine electron microscopic picture of the mitochondrial cloud in stage I oocytes. The mitochondrial cloud includes a large number of mitochondria (arrowheads) and other organelles such as endoplasmic reticulum (arrows). Mitochondria occupied about 42% of whole area presented. Scale bar represents 200 nm (B). Protein profile in gradient SDS-PAGE (C). Red arrows show bands that indicated a lower protein level in stage I sample than stage VI sample. The 8, 21, and 23 bands were identified as F<sub>1</sub>-β, F<sub>0</sub>-b, and F<sub>1</sub>-δ, respectively. Black arrows show bands that were common to two samples. The 12, 14, and 18 bands were identified as GOT, MDH, and AK, respectively. Western blotting (D). F<sub>0</sub>-b and F<sub>1</sub>-β were lower in terms of protein level in stage I sample than in stage VI sample. GOT and MDH were detected at similar levels between stage VI and I samples.

We want to compare the mitochondria from stage VI oocytes and same amount of the mitochondria from mitochondrial cloud. Both samples were standardized by following histological semi-quantification. We estimated the ratio of area that was occupied with mitochondria in mitochondrial cloud, using 5 electron microscopic pictures given from 3 different oocytes. As a result, the ratios of mitochondrial area were 40%, 44%, 44%, 45%, and 47%, giving the average ratio 42%. The area ratio of mitochondria reflects the volume ratio of mitochondria to mitochondrial cloud in one section. As the 5 ratios mentioned above were almost constant, the ratio of mitochondria volume in whole mitochondrial cloud was guessed to be similar to the average ratio of mitochondrial area. Another supposition was that the concentration of protein was similar between mitochondria and the other cytoplasm in mitochondrial cloud. When the stage VI sample was used half the amount of the stage I sample, the mitochondria from stage VI oocytes would be compared with similar amount of mitochondria from mitochondrial cloud.

The highly purified mitochondria from stage VI oocytes represented some major proteins (arrow numbers 1–24 in Fig. 1C). Most of these bands (arrow numbers 1–6, 9–12, 14, 15, 17–20, 24 in Fig. 1C) were similar level between two samples. We found seven bands that indicated a lower amount in the stage I sample than in the stage VI sample (arrow numbers 7, 8, 13, 16, 21, 22, 23 in Fig. 1C).

These seven bands were further processed for N-terminal sequencing, and three of them were identified as ATP synthase β (F<sub>1</sub>-β), *b* (F<sub>0</sub>-b), and δ (F<sub>1</sub>-δ) (arrow numbers 8, 21, 23 in Fig. 1C). Three major common bands were optionally chosen and identified as glutamate oxaloacetate transaminase2 (GOT), malate dehydrogenase2a (MDH), and adenylate kinase2 (AK) (arrow numbers 12, 14, 18 in Fig. 1C). These proteins generally function in mitochondria of various cells (Donald Voet, 1995). For further analysis, these proteins were used as a standard to compare two samples.



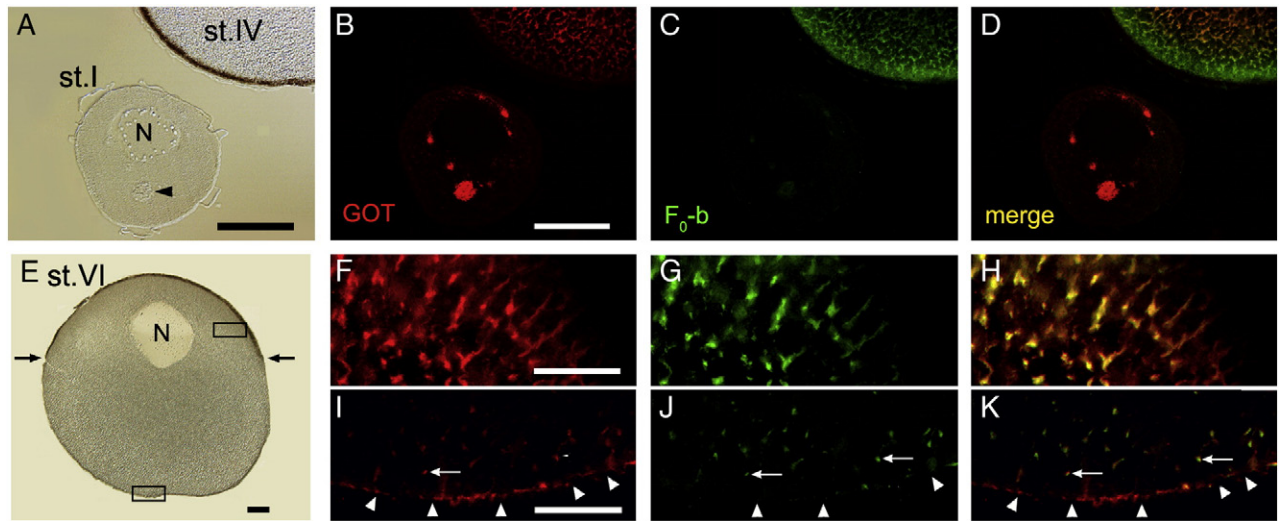


**Fig. 2.** Expression of  $F_0$ -b in stage I and VI oocytes. Sections of ovary double-stained with antibodies against GOT (red) and  $F_0$ -b (green). (A–D) A stage I oocyte in the center of (A) has a mitochondrial cloud (arrowhead) under the nucleus (N). A stage IV oocyte is at the upper right. All mitochondria of the two cells were visualized by anti-GOT (B). All mitochondria in a stage I oocyte were  $F_0$ -b-negative (C, D). Mitochondria in the animal hemisphere of stage IV oocyte were  $F_0$ -b-positive. There was background fluorescence at the peripheral cytoplasm (C, D). (E–H) In a stage VI oocyte, arrows indicate boundary of animal hemisphere with heavy melanin granules and vegetal hemisphere (E). A stage VI oocyte has a large number of mitochondria labeled with anti-GOT in the animal hemisphere (F, upper box of E). Mitochondria were also labeled with anti- $F_0$ -b (G), overlaying GOT staining (H). (I–K) Magnified view of lower box of (E) shows accumulation of mitochondria at the vegetal cortex (arrowheads in I) and a few mitochondria in the inner part (arrows in I). The former was  $F_0$ -b-negative, and the latter was  $F_0$ -b-positive (J, K). Scale bars represent 100  $\mu$ m in (A, B, E) and 50  $\mu$ m in (F, I).

To detect each protein specifically, we made antibodies against GOT, MDH,  $F_0$ -b, and  $F_1$ - $\beta$ . Stage I sample was compared with stage VI sample by Western blotting on the same membrane. GOT and MDH were at similar levels between stage I and VI samples as expected. The amounts of  $F_0$ -b and  $F_1$ - $\beta$  in the stage I sample were lower than those of the stage VI sample (Fig. 1D). That is, low levels of  $F_0$ -b and  $F_1$ - $\beta$  were also confirmed by Western blotting.

*All mitochondria in stage I oocytes are  $F_0$ -b-negative, and mitochondria in vegetal cortex of stage VI oocytes are  $F_0$ -b-negative*

To examine whether mitochondria of germ plasm lack ATP synthase, we immunostained oocytes using anti-GOT and anti- $F_0$ -b

antibodies. Anti-GOT antibodies were used to detect mitochondria (Fig. 2B, F, I). In stage I oocytes, most mitochondria were localized in the mitochondrial cloud, some mitochondria surrounded the nucleus as clusters, and a few were scattered in the rest of the cytoplasm (Fig. 2A, B). Unexpectedly, not only the mitochondrial cloud but also the other mitochondria were  $F_0$ -b-negative (Fig. 2B–D). In animal hemisphere of stage VI oocytes, there were a large number of mitochondria (Fig. 2E, F) and they were  $F_0$ -b-positive (Fig. 2F–H). A few mitochondria were present in the inner part of the vegetal hemisphere, and they were  $F_0$ -b-positive (arrows in Fig. 2I–K). In contrast, mitochondria in the vegetal cortex, including germ plasm, were  $F_0$ -b-negative (arrowheads in Fig. 2I–K). The  $F_0$ -b-negative area was spread over the whole cortex of the vegetal hemisphere

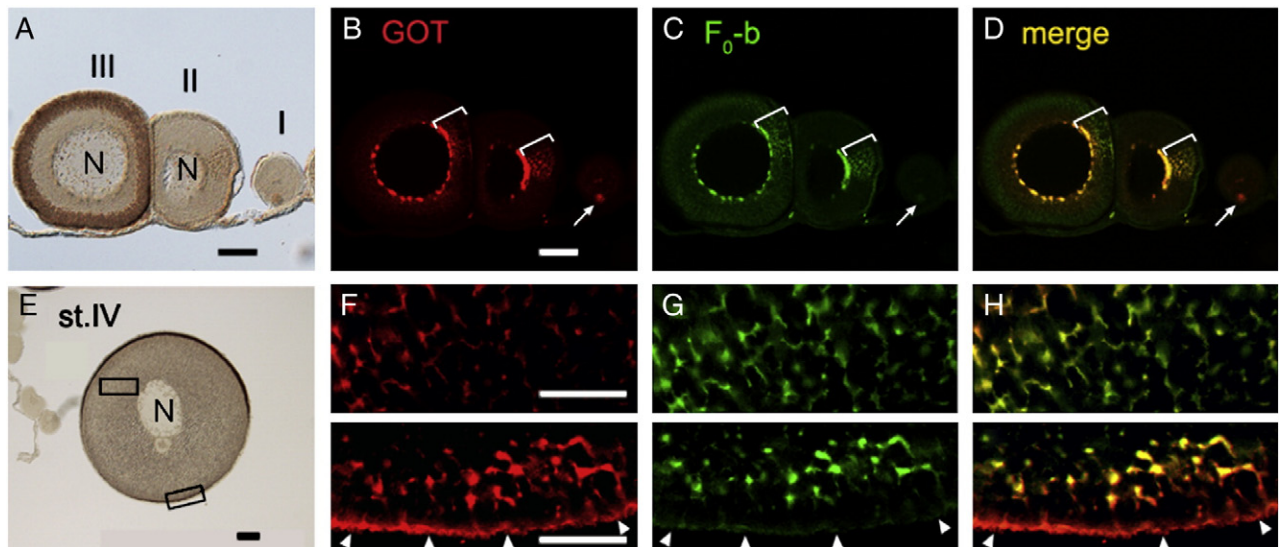


**Fig. 3.** Expression of  $F_0$ -b during oogenesis. (A–D) Stage I, II, and III oocytes are shown in order from right to left (A). The mitochondrial cloud of stage I oocyte (arrow) and fragmented clouds in stage II and III oocytes (brackets) were localized at the vegetal cortex from the nucleus (N) (B). All mitochondria of a stage I oocyte were  $F_0$ -b-negative, and all mitochondria in stage II and III oocytes were  $F_0$ -b-positive (C, D). (E–H) A stage IV oocyte (E) has a large number of mitochondria marked with anti-GOT in the animal hemisphere (F, upper box of E). Mitochondria were also labeled with anti- $F_0$ -b (G), overlaying GOT staining (H). (I–K) Magnified view of lower box of (E) shows mitochondria at the vegetal cortex (arrowheads in I) and mitochondria in the inner part (I). The former became  $F_0$ -b-negative and the latter remained  $F_0$ -b-positive (J, K). Scale bars represent 100  $\mu$ m in (A, B, E) and 50  $\mu$ m in (F, I).



(Fig. 2E). Namely, the  $F_0$ -b-negative area was not limited to the germ plasm.

#### Expression of $F_0$ -b changes dramatically during oogenesis

Distributions of  $F_0$ -b-negative mitochondria in the two stages were different. We examined how the expression of  $F_0$ -b changes in mitochondria of germ plasm during oogenesis. In stage II and III oocytes (Fig. 3A), the mitochondrial cloud was fragmented, and patches of mitochondrial cloud moved towards the vegetal cortex. In addition, mitochondria increased in number around the nucleus and in the rest of the cytoplasm (Fig. 3B). In stage II and III oocytes, all mitochondria were  $F_0$ -b-positive (Fig. 3C, D). In the stage IV oocytes (Fig. 3E), mitochondria in the vegetal cortex including germ plasm became  $F_0$ -b-negative (arrowheads in Fig. 3I–K). The  $F_0$ -b-negative area was spread over the whole cortex of the vegetal hemisphere. A few mitochondria were present in the inner part of the vegetal hemisphere, and they remained  $F_0$ -b-positive. In the animal hemisphere, mitochondria were  $F_0$ -b-positive (Fig. 3F–H).

#### COX activity changes dramatically during oogenesis

Immunostaining analysis showed that the expression of ATP synthase changed during oogenesis. ATP synthase uses the energy of the  $H^+$  gradient to synthesize ATP. An electrochemical proton

gradient across the inner mitochondrial membrane is produced by three respiratory enzyme complexes I, III, and IV (COX). It is assumed that  $F_0$ -b-negative mitochondria also exhibit low electron transport activity. We detected COX activity histochemically at the ultrastructural level, using DAB as a substrate. The intensity of staining by oxidized DAB in the intracristae space of mitochondria corresponds with COX activity. After controls were treated with KCN, which inhibits COX activity, no stages of oocytes were stained with DAB (Fig. 4A'–J'). We also paid attention to mitochondrial morphology.

In stage I oocytes, mitochondria in the mitochondrial cloud and the other parts of the cytoplasm were short with very poor cristae (Fig. 4B', A'), showing no COX activity (Fig. 4B, A). In early stage II oocytes, the mitochondrial cloud was initiated to spread from the peri-nuclear space to the vegetal cortex. Some mitochondria became long, with developed cristae (Fig. 4C', D'), and all mitochondria showed high COX activity (Fig. 4C, D). In late stage II and III oocytes, the mitochondrial cloud was fragmented further. Mitochondria in the vegetal hemisphere including the fragmented mitochondrial cloud showed morphology similar to that of early stage II oocytes (Fig. 4F, F'). Their COX activity was heterogeneous in the population and also in areas of one mitochondrion (Fig. 4F). In the animal hemisphere, many mitochondria formed a tubular network, with developed cristae (Fig. 4E'), and showed high COX activity (Fig. 4E). In stage IV–VI oocytes, mitochondria in the vegetal cortex including germ plasm were short, with narrow cristae (Fig. 4H', J'). They

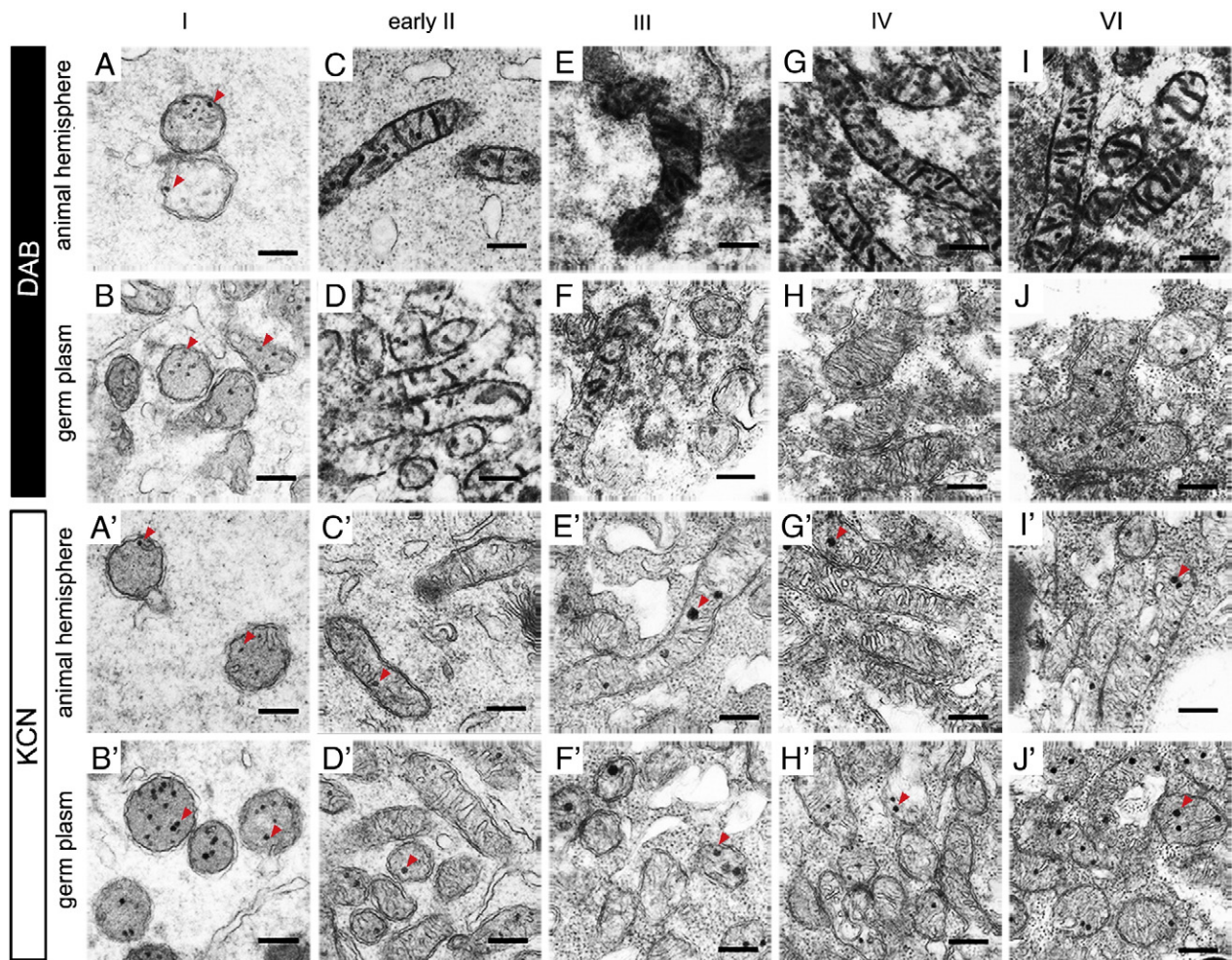


**Fig. 4.** Ultrastructural analysis of oocytes on COX activity during oogenesis. (A'–J') KCN inhibits COX activity in all stages of oocytes. Dense granules (arrowheads) are mitochondrial granules, not reaction products. (A, B) No mitochondria in stage I oocytes showed COX activity. (C, D) All mitochondria in early stage II oocytes showed high COX activity. (F, H, J) COX activity was heterogeneous in the population and also in areas of one mitochondrion at the vegetal hemisphere of stage III oocytes (F). Mitochondria at the vegetal cortex showed no COX activity in stage IV (H) and VI oocytes (J). (E, G, I) Mitochondria in the animal hemisphere showed high COX activity. Scale bars represent 200 nm.

showed no COX activity (Fig. 4H, J). The area of mitochondria with no COX activity was spread over the whole cortex of the vegetal hemisphere. In the animal hemisphere, mitochondria formed tubular network, with developed cristae (Fig. 4G', I'). They showed high COX activity (Fig. 4G, I).

It was shown that COX activity was correlated with expression of ATP synthase at almost all stages of oocytes. Respiratory activity and mitochondrial morphology changed dramatically during oogenesis.

## Discussion

### *The whole ATP synthase is low in mitochondria at stage I oocytes*

We have investigated the characteristics of mitochondria transmitted to the next generation. We compared the protein profiles between germ-line and somatic mitochondria and found only 7 bands down regulated in stage I sample, because of limitation in resolution by our SDS-PAGE. Among them, the levels of subunits of ATP synthase, F<sub>0</sub>-b, F<sub>1</sub>-β, and F<sub>1</sub>-δ, were low in germ-line mitochondria. ATP synthase is an enzyme that is comprised of two functional components, F<sub>1</sub> and F<sub>0</sub> (Garcia-Trejo and Morales-Rios, 2008), and both components are needed for OXPHOS. As both F<sub>0</sub> and F<sub>1</sub> subunits were present at low protein levels in the stage I sample, the whole level of ATP synthase might be low at this stage. Furthermore, other respiratory chain complexes may be low at protein level, as follows.

The mtDNA codes for 13 polypeptides, all of which are subunits of the respiratory chain complexes (Complex I, III, COX, and ATP synthase). The majority of the subunit that forms the respiratory chain complexes is encoded by nuclear DNA. The functional respiratory chain complexes are formed from both peptides encoded by mtDNA and nuclear DNA.

The subunits encoded by mtDNA are core for respiratory chain complexes. They represent the starting points of protein complex assembly, and their expression is tightly regulated because mis-assembled subunits harbor the danger of ROS (Fontanesi et al., 2006; Mick et al., 2010). That is, the amount of core complexes inserted into the inner mitochondrial membrane is rate limiting for expression of the other surrounded subunits. We suggest that whole respiratory chain complexes are down regulated in mitochondria of stage I oocytes as ATP synthase.

### *High respiratory activity is temporary during oogenesis in mitochondria of the germ plasm*

We examined the intracellular distribution of ATP synthase during oogenesis. In stage I oocytes, not only germ plasm mitochondria but also non-germ plasm mitochondria were ATP synthase-negative. In stage II and III oocytes, all mitochondria in the cytoplasm including germ plasm were ATP synthase-positive. In stage IV–VI oocytes, mitochondria in the germ plasm became ATP synthase-negative again. We investigated the activity of COX using DAB staining to determine whether enzymes upstream of ATP synthase are active or not. With the exception of stage II–III oocytes, the expression of ATP synthase was correlated with COX activity during oogenesis. In stage II–III oocytes, ATP synthase was positive in all mitochondria. COX activity was high in all mitochondria only in early stage II oocytes as the mitochondrial cloud initiated migration. In late stage II and III oocytes, COX activity of mitochondria in the vegetal hemisphere was heterogeneous in the population and also in areas of one mitochondrion. At these stages, heterogeneous activity of COX seems to disagree with the uniform expression of ATP synthase. Ultrastructural histochemistry with DAB may show precise respiratory activity in each mitochondrion rather than immunostaining at light microscopy. High respiratory activity was temporary in mitochondria of the germ plasm.

### *Mitochondrial morphology reflects expression of ATP synthase and COX activity*

Mitochondria change their morphology for network formation and development of cristae in response to their respiratory activity. Yeast Mgm1 or its mammalian homolog OPA1 has mitochondrial fusion activity when mitochondrial ATP level or mitochondrial inner membrane potential ( $\Delta\psi$ ) is high and induces filamentous mitochondrial structures. When mitochondrial ATP level and  $\Delta\psi$  is low, these molecules lose fusion stimulating activity and induce mitochondrial fragmentation (Herlan et al., 2004; Ishihara et al., 2006). When ATP synthase alters from oligomeric form to monomeric form, the cristae morphology alters (Arselin et al., 2004). Mitochondria have open cristae when they are active, but they have narrow cristae when they are inactive (Hackenbrock, 1966). In stage I oocytes, mitochondrial morphology was found to be short, with very poor cristae. In stage IV–VI oocytes, mitochondria of vegetal cortex including germ plasm were short, with narrow cristae. These morphologies may reflect low COX activity and a low level of ATP synthase. On the other hand, mitochondria in the animal hemisphere of stage IV–VI oocytes were long, with open cristae. This may reflect high COX activity and a high level of ATP synthase.

### *Stage I oocytes contain only germ-line mitochondria*

At first, mitochondrial cloud in stage I oocytes is supposed to comprise germ-line mitochondria, because it also contains germinal granules responsible for future germ cell formation. The mitochondria scattered in the other cytoplasm of stage I oocytes were not expected to be germ-line mitochondria.

After completion of immunological and ultrastructural examination, unexpectedly, not only mitochondrial cloud but also the other mitochondria were suppressed in respiration. We reconsidered our first premise. Our present premise is that the stage I oocytes contain only germ-line mitochondria.

Stage I oocytes just inherit germ-line mitochondria and may not have somatic ones, yet. After stage II oocytes, the large number of mitochondria is produced from germ-line mitochondria. Germ-line mitochondria move towards the vegetal cortex, together with mRNAs responsible for future germ cell formation, along with message transport organizer (METRO) pathway (Kloc et al., 2001). As a result, mitochondria are segregated into germ-line mitochondria and somatic ones.

### *Inactive mitochondria of vegetal cortex in stage IV–VI are related to germ plasm*

In stage IV–VI oocytes, the mitochondria with low respiratory activity, that is, inactive mitochondria, were spread over the whole cortex of the vegetal hemisphere. However, germ-plasm-specific molecules, such as *Xcat2*, *Xpat*, and *Xdazl*, were shown to be localized in the vegetal pole (Houston et al., 1998; Hudson and Woodland, 1998; Mosquera et al., 1993). After maturation and successive fertilization, the mitochondria that were spread over the whole vegetal cortex were found to move to the vegetal pole of the egg, forming small patches of mitochondria (Czolowska, 1969; Quaas and Wylie, 2002). During the cleavage stage, the patches of mitochondria in the cortex of the vegetal pole accompany mRNAs specific to germ plasm. Inactive mitochondria of the vegetal cortex in stage IV–VI seem to be related to germ plasm.

### *Suppression of respiratory activity may contribute to maintain germ-line mitochondria accurately from generation to generation*

It is especially noticeable that the respiratory activity of germ-line mitochondria was suppressed in most of the stages during oogenesis.



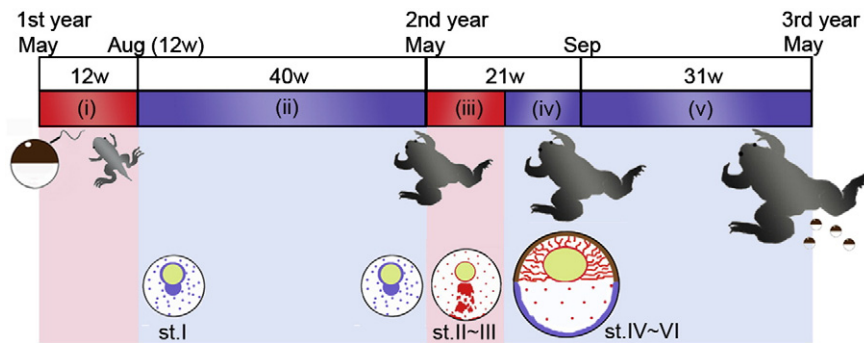


**Fig. 5.** Scheme showing relationship between frog development and respiratory activity of germ-line mitochondria. Gametogenesis is divided into 5 phases based on the change in respiratory activity of germ-line mitochondria (i–v). (i) Respiratory activity is high during embryo and early tadpole stages. Respiratory activity is not decided during late tadpole and young froglet stages. (ii) Respiratory activity is low during froglet stage with stage I oocytes. (iii–iv) From the second year, oocytes grow from stage I to VI, taking 21 weeks. The respiratory activity becomes high in only stage II–III oocytes (iii) and becomes low in germ-line mitochondria in stage IV–VI oocytes (iv). Duration of phase (iii) is not clear. (v) Respiratory activity is low in germ-line mitochondria from the second autumn to the third spring. As a whole, low respiratory activity in germ-line mitochondria contributes to their accurate maintenance through generations.

The biological meaning of this may be discussed on the basis of the developmental schedule and seasonal breeding of *X. laevis*. There are few reports on oogenesis from embryo to mature frog in the field (Gatenby, 1916; Grant, 1953; Ogielska and Kotusz, 2004). The basic type of gametogenesis among frogs is represented by *Rana temporaria* and also *X. laevis* (Ogielska and Kotusz, 2004). Gametogenesis is divided into 5 phases based on the change of respiratory activity that we have found (Fig. 5). (i) From fertilization in spring (March) to early tadpole (2 weeks), primordial germ cells (PGCs) appear in the embryo and move to the gonads. Germ-line mitochondria are active at this stage (Fig. S1, 2). From late tadpole to young froglet (2–12 weeks), the activity of germ-line mitochondria is not decided. (ii) Ovary is filled with oocytes containing the mitochondrial cloud (stage I oocytes in *X. laevis*) at around 12 weeks (Ogielska and Kotusz, 2004). Oocytes remain at stage I until the spring of the second year for more than 40 weeks. In phase (ii), germ-line mitochondria are inactive. (iii–iv) From spring (March) to early autumn (September) of the second year (about 21 weeks), oocytes accumulate yolk (stage II–VI oocytes in *X. laevis*) (Gatenby, 1916; Grant, 1953). It is not clear how long the oocytes spend at each oogenetic stage. Only in stage II–III oocytes are germ-line mitochondria active (iii). Germ-line mitochondria become inactive in stage IV–VI oocytes (iv). (v) Final oocytes (stage VI oocytes in *X. laevis*) pass through a hibernation stage and are ready for the third spring (Gatenby, 1916; Grant, 1953). In phase (v), germ-line mitochondria are inactive.

In this study, we have shown that germ-line mitochondria are suppressed in terms of respiratory activity in more than 70% of the 2 years during gametogenesis in *X. laevis*. Germ-line mitochondria are only active in phases (i) and (iii). In phase (i), PGCs differentiate. In phase (iii), oocytes accumulate yolk and synthesize organelles, mRNA, rRNA, and so on (Golden et al., 1980; Hill and Macgregor, 1980; Rosbash, 1974; Tourte et al., 1984). In these phases occupying less than 30% of the gametogenetic period, cells have a particular need for ATP. In phase (iv–v), mitochondria increase in number and segregate into somatic mitochondria and germ-line mitochondria; the former function to maintain oocytes, the latter are inactive for the next generation.

Mitochondria contain their own DNA that should be transmitted accurately to progeny. Mitochondria generate the majority of cellular ROS, which may impair mtDNA. In somatic cells, the mitochondrial genome is vulnerable to rapid accumulation of deleterious mutations during an animal's lifetime (Wallace et al., 1995). The mitochondrial genome in animal cells has been conserved throughout evolution. A bottleneck is necessary to limit deleterious mutations in the inherited mitochondrial genome somewhere in oogenesis (Bergstrom and Pritchard, 1998; Cao et al., 2007; Cree et al., 2008; Hauswirth and Laipis, 1982; Wai et al., 2008). Germ-line mitochondria maintain a low

level of ATP synthase, repress OXPHOS and ROS production, and suppress impairment of mtDNA, so that they are maintained accurately from generation to generation. There may be some mechanisms to suppress respiration in germ-line mitochondria in any organisms that have symbiosis-established mitochondria.

Supplementary materials related to this article can be found online at doi:10.1016/j.ydbio.2010.11.021.

## Acknowledgments

This work was partly supported by KAKENHI (19-55531) and Sasakawa Scientific Research Grant from the Japan Science Society. We are very grateful to Dr. T. Takahashi (Tokyo University, Present address: Toyama Chemical Co., Ltd.) and M. Furutani (Okayama University) for their excellent technical support. We also thank other members of our laboratory for their support.

## References

- Altschul, S.F., Madden, T.L., Schaffer, A.A., Zhang, J., Zhang, Z., Miller, W., Lipman, D.J., 1997. Gapped BLAST and PSI-BLAST: a new generation of protein database search programs. *Nucleic Acids Res.* 25, 3389–3402.
- Arselin, G., Vaillier, J., Salin, B., Schaeffer, J., Giraud, M.F., Dautant, A., Brethes, D., Velours, J., 2004. The modulation in subunits e and g amounts of yeast ATP synthase modifies mitochondrial cristae morphology. *J. Biol. Chem.* 279, 40392–40399.
- Bergstrom, C.T., Pritchard, J., 1998. Germline bottlenecks and the evolutionary maintenance of mitochondrial genomes. *Genetics* 149, 2135–2146.
- Bogenhagen, D.F., Wang, Y., Shen, E.L., Kobayashi, R., 2003. Protein components of mitochondrial DNA nucleoids in higher eukaryotes. *Mol. Cell. Proteomics* 2, 1205–1216.
- Cao, L., Shitara, H., Horii, T., Nagao, Y., Imai, H., Abe, K., Hara, T., Hayashi, J., Yonekawa, H., 2007. The mitochondrial bottleneck occurs without reduction of mtDNA content in female mouse germ cells. *Nat. Genet.* 39, 386–390.
- Chan, A.P., Kloc, M., Etkin, L.D., 1999. fatvg encodes a new localized RNA that uses a 25-nucleotide element (FVLE1) to localize to the vegetal cortex of *Xenopus* oocytes. *Development* 126, 4943–4953.
- Cohen, S., Pante, N., 2005. Pushing the envelope: microinjection of Minute virus of mice into *Xenopus* oocytes causes damage to the nuclear envelope. *J. Gen. Virol.* 86, 3243–3252.
- Cree, L.M., Samuels, D.C., de Sousa Lopes, S.C., Rajasimha, H.K., Wonnapijit, P., Mann, J.R., Dahl, H.H., Chinnery, P.F., 2008. A reduction of mitochondrial DNA molecules during embryogenesis explains the rapid segregation of genotypes. *Nat. Genet.* 40, 249–254.
- Czolowska, R., 1969. Observations on the origin of the 'germinal cytoplasm' in *Xenopus laevis*. *J. Embryol. Exp. Morphol.* 22, 229–251.
- Donald Voet, J.G.V., 1995. *Biochemistry*. John Wiley & Sons, Inc.
- Dumont, J.N., 1972. Oogenesis in *Xenopus laevis* (Daudin). I. Stages of oocyte development in laboratory maintained animals. *J. Morphol.* 136, 153–179.
- Fontanesi, F., Soto, I.C., Horn, D., Barrientos, A., 2006. Assembly of mitochondrial cytochrome c-oxidase, a complicated and highly regulated cellular process. *Am. J. Physiol. Cell Physiol.* 291, C1129–C1147.
- Garcia-Trejo, J.J., Morales-Rios, E., 2008. Regulation of the F(1)F(0)-ATP synthase rotary nanomotor in its monomeric-bacterial and dimeric-mitochondrial forms. *J. Biol. Phys.* 34, 197–212.
- Gatenby, J.B., 1916. The transition of peritoneal epithelial cells into germ cells in some amphibia anura, especially in *Rana temporaria*. *Q. J. Microsc. Sci.* 61, 275–300.

- Golden, L., Schafer, U., Rosbash, M., 1980. Accumulation of individual pA + RNAs during oogenesis of *Xenopus laevis*. *Cell* 22, 835–844.
- Grant, P., 1953. Phosphate metabolism during oogenesis in *Rana temporaria*. *J. Exp. Zool.* 124, 513–543.
- Hackenbrock, C.R., 1966. Ultrastructural bases for metabolically linked mechanical activity in mitochondria. I. Reversible ultrastructural changes with change in metabolic steady state in isolated liver mitochondria. *J. Cell Biol.* 30, 269–297.
- Hauswirth, W.W., Laipis, P.J., 1982. Mitochondrial DNA polymorphism in a maternal lineage of Holstein cows. *Proc. Natl Acad. Sci. USA* 79, 4686–4690.
- Heasman, J., Quarmby, J., Wylie, C.C., 1984. The mitochondrial cloud of *Xenopus* oocytes: the source of germinal granule material. *Dev. Biol.* 105, 458–469.
- Herlan, M., Bornhovd, C., Hell, K., Neupert, W., Reichert, A.S., 2004. Alternative topogenesis of Mgm1 and mitochondrial morphology depend on ATP and a functional import motor. *J. Cell Biol.* 165, 167–173.
- Hill, R.S., Macgregor, H.C., 1980. The development of lampbrush chromosome-type transcription in the early diplotene oocytes of *Xenopus laevis*: an electron-microscope analysis. *J. Cell Sci.* 44, 87–101.
- Houston, D.W., Zhang, J., Maines, J.Z., Wasserman, S.A., King, M.L., 1998. A *Xenopus* DAZ-like gene encodes an RNA component of germ plasm and is a functional homologue of *Drosophila* boule. *Development* 125, 171–180.
- Hudson, C., Woodland, H.R., 1998. Xpat, a gene expressed specifically in germ plasm and primordial germ cells of *Xenopus laevis*. *Mech. Dev.* 73, 159–168.
- Ikeuchi, M., Takio, K., Inoue, Y., 1989. N-terminal sequencing of photosystem II low-molecular-mass proteins. 5 and 4.1 kDa components of the O<sub>2</sub>-evolving core complex from higher plants. *FEBS Lett.* 242, 263–269.
- Ishihara, N., Fujita, Y., Oka, T., Mihara, K., 2006. Regulation of mitochondrial morphology through proteolytic cleavage of OPA1. *EMBO J.* 25, 2966–2977.
- Ito, H., Saito, Y., Watanabe, K., Orii, H., 2001. Epimorphic regeneration of the distal part of the planarian pharynx. *Dev. Genes Evol.* 211, 2–9.
- Kashino, Y., 2003. Separation methods in the analysis of protein membrane complexes. *J. Chromatogr. B Analyt. Technol. Biomed. Life Sci.* 797, 191–216.
- Kashino, Y., Koike, H., Satoh, K., 2001. An improved sodium dodecyl sulfate-polyacrylamide gel electrophoresis system for the analysis of membrane protein complexes. *Electrophoresis* 22, 1004–1007.
- Kataoka, K., Yamaguchi, T., Orii, H., Tazaki, A., Watanabe, K., Mochii, M., 2006. Visualization of the *Xenopus* primordial germ cells using a green fluorescent protein controlled by cis elements of the 3' untranslated region of the DEADSouth gene. *Mech. Dev.* 123, 746–760.
- Kloc, M., Bilinski, S., Chan, A.P., Allen, L., Zearfoss, N.R., Etkin, L.D., 2001. RNA localization and germ cell determination in *Xenopus*. *Int. Rev. Cytol.* 203, 63–91.
- Mick, D.U., Vukotic, M., Piechura, H., Meyer, H.E., Warscheid, B., Deckers, M., Rehling, P., 2010. Coa3 and Cox14 are essential for negative feedback regulation of COX1 translation in mitochondria. *J. Cell Biol.* 191, 141–154.
- Mosquera, L., Forristall, C., Zhou, Y., King, M.L., 1993. A mRNA localized to the vegetal cortex of *Xenopus* oocytes encodes a protein with a nanos-like zinc finger domain. *Development* 117, 377–386.
- Ogielska, M., Kotusz, A., 2004. Pattern and rate of ovary differentiation with reference to somatic development in anuran amphibians. *J. Morphol.* 259, 41–54.
- Orii, H., Ito, H., Watanabe, K., 2002. Anatomy of the planarian *Dugesia japonica* I. The muscular system revealed by antisera against myosin heavy chains. *Zool. Sci.* 19, 1123–1131.
- Quaas, J., Wylie, C., 2002. Surface contraction waves (SCWs) in the *Xenopus* egg are required for the localization of the germ plasm and are dependent upon maternal stores of the kinesin-like protein Xklp1. *Dev. Biol.* 243, 272–280.
- Rosbash, M., 1974. Polyadenylic acid-containing RNA in *Xenopus laevis* oocytes. *J. Mol. Biol.* 85, 87–101.
- Sacccone, C., Gissi, C., Reyes, A., Larizza, A., Sbisa, E., Pesole, G., 2002. Mitochondrial DNA in metazoa: degree of freedom in a frozen event. *Gene* 286, 3–12.
- Seligman, A.M., Karnovsky, M.J., Wasserkug, H.L., Hanker, J.S., 1968. Nondroplet ultrastructural demonstration of cytochrome oxidase activity with a polymerizing osmiophilic reagent, diaminobenzidine (DAB). *J. Cell Biol.* 38, 1–14.
- Takahashi, T., Kuroiwa, S., Ogura, T., Yoshikawa, S., 2005. Probing the oxygen activation reaction in intact whole mitochondria through analysis of molecular vibrations. *J. Am. Chem. Soc.* 127, 9970–9971.
- Tourte, M., Mignotte, F., Mounolou, J.C., 1984. Heterogeneous distribution and replication activity of mitochondria in *Xenopus laevis* oocytes. *Eur. J. Cell Biol.* 34, 171–178.
- Wai, T., Teoli, D., Shoubridge, E.A., 2008. The mitochondrial DNA genetic bottleneck results from replication of a subpopulation of genomes. *Nat. Genet.* 40, 1484–1488.
- Wallace, D.C., Shoffner, J.M., Trounce, I., Brown, M.D., Ballinger, S.W., Corral-Debrinski, M., Horton, T., Jun, A.S., Lott, M.T., 1995. Mitochondrial DNA mutations in human degenerative diseases and aging. *Biochim. Biophys. Acta* 1271, 141–151.
- Wu, G.J., Dawid, I.B., 1972. Purification and properties of mitochondrial deoxyribonucleic acid dependent ribonucleic acid polymerase from ovaries of *Xenopus laevis*. *Biochemistry* 11, 3589–3595.